The Bioscan
AN INTERNATIONAL QUARTERLY JOURNAL OF LIFE SCIENCES
20(4): 421-441, 2025 www.thebioscan.com

Pareto Optimization–based Nonsubsampled Contourlet Transform (NSCT) Medical Image Compression

[1]Mrs. C. Nandhini, [2]Dr. G. Vijaiprabhu

[1]Research Scholar, PG and Research Department of Computer Science, Erode Arts and Science College (Autonomous), Erode, Tamilnadu,India. Email: ashonanthu@gmail.com

[2]Assistant Professor, PG and Research Department of Computer Science, Erode Arts and Science College (Autonomous), Erode, Tamilnadu,India. Email: gvprabhu7@gmail.com

DOI: 10.63001/tbs.2025.v20.i04.pp421-441

KEYWORDS:
Compression, NSCT, Pareto, Optimization, Distortion, Fidelity, PSNR, Classification, and medical image.

Received on:

25-08-2025

Accepted on:

30-09-2025

Published on:

17-11-2025

ABSTRACT

The exponential growth of medical imaging data from modalities such as MRI, CT, and X-ray poses significant challenges for storage, transmission, and real-time analysis in clinical settings. Conventional compression techniques, including JPEG, JPEG2000, and wavelet-based methods, often fail to preserve fine anatomical and pathological structures critical for accurate diagnosis. This study proposes a Pareto Optimization–based Nonsubsampled Contourlet Transform (PO-NSCT) framework for medical image compression, integrating multi-scale and multi-directional decomposition with evolutionary multi-objective optimization. The compression process is formulated as a multi-objective problem to simultaneously minimize distortion (MSE), maximize compression ratio (CR), and preserve structural fidelity (SSIM). NSGA-II is employed to identify Pareto-optimal parameter configurations, enabling a systematic trade-off between rate and image quality. Experimental evaluation is conducted on 7,023 brain MRI images from Figshare, SARTAJ, and Br35H datasets. Results demonstrate that PO-NSCT outperforms existing methods, achieving higher compression ratios (up to 65.7%) with superior PSNR (>38 dB) and SSIM (>0.95), while enhancing downstream classification accuracy by 5–10%. Statistical validation via Wilcoxon signed-rank tests confirms significance ($p < 0.05$). The framework preserves diagnostically relevant features, ensuring clinical reliability, scalability, and suitability for telemedicine and AI-assisted workflows.

Introduction

Medical imaging has experienced an enormous revolution in recent decades, influenced by the development of imaging techniques including computed tomography (CT), magnetic resonance imaging (MRI), positron emission tomography (PET), and ultrasound. Such modalities are now essential in the diagnosis, treatment planning and long-term follow-ups of patients in a broad spectrum of clinical areas such as oncology, neurology, cardiology and orthopedics [1]. The growing use of imaging in the context of precision medicine and evidence-based clinical decision-making has resulted in an exponential increase in the amount of medical images produced every day in hospitals and diagnostic facilities. This unsurpassed increase in data is presenting critical challenges to healthcare systems as far as storage, retrieval, transmission, and real-time analysis of medical images are concerned [2].

One of the basic ways to address these issues is to come up with effective medical image compression algorithms [3]. By compressing data, compression helps achieve a smaller data footprint, which facilitates the efficient use of storage resources, a more rapid transmission across a network bandwidth constraint, and a smooth integration of imaging data into telemedicine and cloud-based healthcare systems. Medical images however, are not the same as natural images because they have high diagnostic value and a need to preserve delicate anatomical and pathological structures. Indeed, medical image compression should strike a fine balance between file size and diagnostic content [4]. The deterioration of image quality affecting clinical interpretation can have dire consequences to patient safety and medical image compression is a much more demanding task than natural photograph compression [4].

Conventional image compression techniques like JPEG, JPEG2000 and Set Partitioning in Hierarchical Trees (SPIHT) utilise representations in the transform domain to minimise redundancy in image data. Though these methods have worked well in some settings, they tend to produce an incomplete image of the medical image due to their inability to capture the complex geometric and directional features of the medical image [5]. Such insufficiency may lead to the loss of important features, especially edges and fine textures used in the detection of small lesions, microcalcifications, or even subtle tissue abnormalities [6]. To overcome these drawbacks, an alternative approach called Nonsubsampled Contourlet Transform (NSCT) has become a promising method in the representation as well as compression of medical images [7]. The NSCT is a flexible, multiscale, and multidirectional image decomposition that is shift-invarient and has better directional sensitivity. This allows modeling edges, contours, and fine anatomical features effectively and therefore diagnostic content is preserved even at the time of compression [8].

Although the theory of NSCT has its benefits, it is not a simple matter to implement in medical imaging compression [9]. An NSCT-based compression system is sensitive to many parameters such as the number of decomposition levels, the number of directional subbands per level, the filter bank used, the thresholding method, and the size of the quantization steps used on the transform coefficients. The combination of these parameters is used to decide the trade-off between compression ratio and image fidelity [10]. Manual tuning or heuristic determination of correct parameter values is highly inefficient and suboptimal, especially since the goals of optimization of compression efficiency and retention of diagnostic accuracy are incompatible with each other [11]. The complex needs of clinical imaging applications cannot be sufficiently addressed with a single-objective optimization framework that focuses on either compression ratio or quality [12].

This problem requires the implementation of multi-objective optimization models, which are able to work on multiple goals of performance and offer a set of solutions that reflect various trade-offs. Pareto optimization has become one of the potent paradigms

among such frameworks. Pareto optimization does not seek to balance conflicting objectives into one scalar form, but rather finds a collection of nondominated solutions called the Pareto front. The solutions in the Pareto front represent the various trade-offs between the objectives, e.g., compression ratio and image quality, without any solution being worse than any other solution in any dimension. This strategy gives system designers and clinicians flexibility to choose solutions depending on particular clinical needs or application scenarios.

The reason behind the integration of Pareto optimization in NSCT based medical image compression is thus two-fold. First, the increasing volume of medical imaging data requires compression methods that are both efficient and scalable and versatile across imaging modalities. To take just a few examples, MRI scans tend to have high-frequency structural information, whereas CT images tend to focus on density transitions; a single-size-fits-all compression configuration is not sufficient. Second, it is of utmost importance that diagnostic content is preserved. Small distortions in areas of clinical interest may result in misdiagnosis or a lack of certainty in the decision. Traditional techniques of fixed trade-off do not meet this need. The Pareto optimization is a formalized approach to the exploration of the multidimensional design space of NSCT parameters, as well as to the determination of optimal solutions, taking into account rate, distortion, and clinical fidelity.

This study aims to meet the urgent needs of the medical imaging field and the peculiarities of applying NSCT to Pareto optimization. The former aims to develop a compression system, which operates on the idea of NSCT, that can capture geometric and anatomical features effectively in various medical imaging modes. The second objective is to model the compression process as a multi-objective optimization problem with competing objectives of minimum distortion and maximum compression ratio, and structural similarity and diagnostic interpretability constraints. The third goal is to apply evolutionary multi-objective optimization methods, e.g., Non-dominated Sorting Genetic Algorithm II (NSGA-II) to find Pareto-optimal parameter settings of the NSCT-based compression. This guarantees strong coverage of the parameter space and high quality solutions. The study will focus on delivering a clinically interpretable compression results, i.e. finding solutions of Pareto-optimum, which do not compromise diagnostic utility under various clinical constraints, such as telemedicine or long-term storage context, in which compression ratio is ranked higher.

The urgency behind this study is that medical image compression will play a critical role in the age of big data and precision medicine because it is both efficient and clinically reliable. The proposed research aims at elevating the medical image compression state of art by balancing PO-NSCT with Pareto optimization to ensure that the proposed solution is not only technically viable and efficient, but also clinically relevant. A scalable, high-fidelity, and application-aware compression strategy in the medical imaging field is another major stride of the introduction of Multi-objective

optimization in PO-NSCT-based compression.

Related Works

Research in image compression has seen a shift in paradigm to more sophisticated learning-based and hybrid frameworks not necessarily built using the transform. The increasing requirements of high-resolution medical imaging and the skyrocketing development of storage and transmission structures demand compression algorithms with guarantees of effectiveness as well as diagnostic accuracy. Seasoned methods like wavelet-based or transform-based compression have been a starting point of mathematical theory but tend to miss subtle operational images important in clinical usage.

Recent progress with neural architecture, variational autoencoders (VAEs), and vectors quantization has shown tremendous gains in rate-distortion optimization and flexibility. Furthermore hybrid methods that combine a variety of transforms (e.g., DWT and PCA, or wavelets and entropy models) have attempted to tradeoff between computation speed and faithfulness. Similarly, quantum-inspired methods have come into existence, which provides a visionary way in considering both compression and encryption.

In spite of these innovations, a number of challenges still exist such as computational cost, low scalability to real-time clinical settings and a lack of domain-specific validation. The gaps in the available methods should be highlighted in order to generate the basis of more effective frameworks like Pareto-optimized NSCT to compress medical images. In Table 1 below, all the recent compression methods are analyzed in detail, concerning methodology, the main contributions of this research method, and its disadvantages.

Table 1. Comprehensive Analysis of Recent Compression Techniques

Author(s) & Year	Methodology / Algorithm	Key Contribution (Inference)	Drawbacks
Wang, G. H., Li, J., Li, B., & Lu, Y. (2023) [13]	Neural image compression with Mask Decay	Demonstrates real-time neural image compression with efficient rate–distortion trade-off	High computational demand during training; limited testing on medical datasets
Jiang, W., Yang, J., Zhai, Y., Gao, F., & Wang, R. (2023) [14]	MLIC++ with multi-reference entropy modeling	Achieves linear complexity while improving entropy modeling efficiency	Model generalization to high-resolution medical images remains untested

Nagar, M. S. R., & MSRIT, P. (2024) [15]	Wavelet-based multi-image compression	Provides mathematical foundation for wavelet-driven compression in diagnostics	Wavelet methods often lose fine structural details critical in medical imaging
Duan, Z., Lu, M., Ma, J., Huang, Y., Ma, Z., & Zhu, F. (2023) [16]	QARV (Quantization-Aware ResNet VAE)	Improves lossy compression using quantization-aware training integrated with ResNet-VAE	Requires significant computational resources; complexity may hinder real-time deployment
Chen, K. H., & Lin, Y. C. (2023) [17]	Adaptive VQVAE	Introduces adaptability in vector quantized compression, enhancing learned compression	Sensitive to hyperparameter tuning; limited application on domain-specific data
Ma, Y., & Zhou, N. R. (2023) [18]	Quantum Fibonacci Transform for compression and encryption	Integrates compression with encryption, leveraging quantum principles for color images	Quantum implementation is theoretical; lacks practical hardware feasibility
Ranjan, R., & Kumar, P. (2023) [19]	2D DWT + PCA + Huffman Encoding	Improves compression efficiency while preserving fidelity	Performance degrades with complex textures and high-dimensional medical images

The current image compression algorithms demonstrate that they are faced by extremely important drawbacks when assessed through the perspective of medical imaging. Neural-based algorithms include EVC, MLIC++, QARV and Adaptive VQVAE that achieve remarkable rate-distortion efficiency, but they are extremely expensive to compute and do not manifest state-of-the-art validation on medical data where diagnostic fidelity is paramount. Wavelet-based and hybrid methods have mathematical traceability, but usually cannot express fine-scale detail (tumor boundaries and vessel edges) and so lose clinically important detail when highly compressed. What makes quantum-inspired applications conceptually innovative, is not practical in terms of its hardware constraints and lack of scalability. Moreover, the majority of the currently available works assume a single-objective optimization approach, considering compression efficiency alone, or reconstruction quality alone, thus failing to account for the multi-

objectivity of medical image compression, in which storage reduction and diagnostic usability are to be optimized together. They also are rarely included in studies as they do not include a clinical validation or task relevant verification of performance like segmentation accuracy of compressed images, leading to a disconnect between algorithmic and clinical performance. This work presents a Pareto Optimization-based Nonsubsampled Contourlet Transform (NSCT) framework, to solve these problems: maximize compression rate and image quality, retain geometry and anatomy structures with the directional sensitivity of NSCT, and combine statistical, perceptual and clinical measures, in achieving mathematically optimal, and clinically faithful compression.

Proposed Methodology - Pareto Optimization–based Nonsubsampled Contourlet Transform (PO-NSCT) based Compression

An NSCT-based lossy compression pipeline for medical images that optimally trades off compression efficiency and diagnostic image fidelity is designed. It is formulated as a multi-objective optimization (MOO) problem and solve using Pareto optimization to obtain a set of non-dominated transform+quantization parameter vectors.

Primary objectives:

- Minimize distortion D (preserve diagnostically relevant features).
- Minimize bitrate R (maximize compression ratio). Optional tertiary objective: maximize perceptual/structural quality (e.g., maximize SSIM) or minimize structural loss $oss\ 1 - SSIM$.

Let the original grayscale medical image be $I \in \mathbb{R}^{H \times W}$. NSCT decomposition yields a lowpass coarse scale and multiple directional bandpass subbands at several scales (no downsampling). Denote the NSCT analysis operator as $T_{\ominus}(.)$ where $\ominus$ encodes NSCT design choices (number of scales , directional decomposition at each scale d_l, and chosen filter banks).

$$T_{\ominus}(I) = \{c_o, c_{l,k} | l = 1 \dots L, k = 1 \dots d_l\}$$

where c_o: lowpass (coarse) coefficients, $c_{l,k}$: directional subband coefficients at scale l and k direction, and Reconstruction operator $T_{\ominus}^{-1}(.)$ satisfies $T_{\ominus}^{-1}(I)) \approx I$ (exact if no quantization/thresholding).

Define parameter vector x (chromosome) that the optimizer will search:

$$x = [L, d_1, \dots, d_L, filter_{idx}, \tau_0, \{\tau_{L,k}\}, s_0, \{s_{L,k}\}]$$

where $L \in \mathbb{Z}^+$ is number of scales, $d_l \in \mathbb{Z}^+$ is directions per scale, $\text{filter}_{\text{idx}}$ is discrete index selecting directional, pyramid filters from a candidate set, τ_0 is threshold(s) for shrinkage/coeff pruning (one per subband or grouped), and s_0 is quantization step size(s) per subband (scalar real >0). The procedure is given in Algorithm 1.

Algorithm 1. Image Compression

1. Analysis: compute NSCT coefficients $C.\tau_{\ominus}(I)$

2. Thresholding / sparsification: apply soft/hard threshold T_τ on each subband:

$$\tilde{C}_{l,k} = T_{\tau_{l,k}}(C_{l,k}) \qquad T_\tau^{hard}(c) = \begin{cases} c & |c| \geq \tau \\ o & |c| < \tau \end{cases}$$

$$T_\tau^{soft}(c) = sign(c)\max(|c| - \tau, 0).$$

$$\hat{c}_{l,k} = Q_{s_{l,k}}(\hat{c}_{l,k}) = \text{round}\left(\frac{\hat{c}_{l,k}}{s_{l,k}}\right)$$

$$\tilde{C}_{l,k}^{dq} = s_{l,k}, \hat{c}_{l,k}.$$

$$R(x) \approx \frac{1}{HW}\sum_{l,k}\sum_{b} -n_{l,k}(b) log_2 p_{l,k}(b)$$

5. Synthesis: reconstruct compressed image

$$\hat{I} = T_{\ominus}^{-1}(\tilde{C}^{dq}, C_0^{dq}).$$

In medical image compression, multiple conflicting objectives often coexist, such as maximizing compression ratio while preserving diagnostic fidelity. Single-objective optimization approaches are insufficient in this context, as they prioritize one metric at the expense of others. Multi-objective optimization (MOO) provides a systematic framework for simultaneously optimizing multiple criteria. Within this paradigm, Pareto optimization is widely employed to identify a set of nondominated solutions, known as the Pareto front, where no solution can be considered superior across all objectives. Each point on the Pareto front represents a unique trade-off between competing goals, such as rate versus distortion, allowing designers and clinicians to select parameter configurations based on specific application requirements. Evolutionary algorithms, particularly the Non-dominated Sorting Genetic Algorithm II (NSGA-II), are effective for Pareto-based MOO due to their ability to explore complex, high-dimensional parameter spaces, maintain population diversity, and converge toward optimal trade-offs. By integrating Pareto optimization into NSCT-based medical image compression, it becomes possible to achieve a balanced solution set that maximizes compression efficiency while preserving critical anatomical and pathological information, ensuring both technical and clinical reliability.

$$min_{x\in X}\, F(x) = [f_1(x), f_2(x)] \quad s.t. x \in \chi$$

where χ contains bounds and discrete choices (e.g.,$L \in [L_{min}, L_{max}], s_{l,k} \in [S_{min}, S_{max}], \tau \in [\tau_{min}, \tau_{max}]$, , , filter index discrete set). Utilised Pareto dominance wher *x* dominates *y* if $f_i(x) \leq f_i(y)$ for all *i* and strictly less for some *i*. The choice of solver: NSGA-II (practical, widely used)

or MOPSO / SPEA2. The NSGA-II for PO-NSCT-based Medical Image Compression is given in Algorithm 2.

Algorithm 2. NSGA-II for PO-NSCT-based Medical Image Compression

Input:

- Original medical image
- NSCT parameter bounds: number of scales, directions per scale, filter choices, quantization steps, thresholds
- NSGA-II parameters: population size, number of generations, crossover probability, mutation probability

Output:

- Pareto-optimal set of NSCT parameters
- Corresponding compression ratio and image quality metrics

Step 1: Chromosome Encoding

- Represent each candidate solution as a mixed discrete-continuous vector containing:
  - Number of NSCT scales
  - Number of directions per scale
  - Filter index
  - Thresholds for coefficient pruning
  - Quantization steps
- Discrete parameters include number of scales, directions, and filter choice.
- Continuous parameters include thresholds and quantization steps.

Step 2: Initialization

- Generate an initial population randomly within parameter bounds.
- For each candidate, evaluate objectives:
  1. Apply NSCT decomposition using the candidate parameters.
  2. Perform thresholding and quantization on the coefficients.
  3. Reconstruct the compressed image.
  4. Compute the objectives: distortion, compression rate, and optionally structural similarity.

Step 3: Non-dominated Sorting

- Sort the population into different fronts based on Pareto dominance.
- The first front contains solutions that are not dominated by any other solution, the second front contains solutions dominated only by the first front, and so on.

Step 4: Crowding Distance Calculation

- Compute crowding distance within each front to maintain diversity.
- Ensures that the Pareto front covers the entire trade-off space evenly.

Step 5: Selection

- Use binary tournament selection based on Pareto rank and crowding distance to choose parents for the next generation.

Step 6: Genetic Operators

- **Crossover:** Use simulated binary crossover for continuous parameters and uniform or one-point crossover for discrete parameters.
- **Mutation:** Use polynomial mutation for continuous parameters and random perturbation for discrete parameters.
- **Repair:** Clamp all parameters to their valid ranges to ensure feasible NSCT configurations.

Step 7: Population Update

- Combine parent and offspring populations.
- Perform non-dominated sorting on the combined population.
- Select the best individuals based on rank and crowding distance to form the next generation.

Step 8: Termination Criteria

- Stop when the maximum number of generations is reached or when convergence metrics (such as hypervolume) stagnate.

Step 9: Knee Point Selection

- Identify knee points on the final Pareto front to select parameter sets that provide the best trade-off between compression and image quality.

Step 10: Output

- Final Pareto front of non-dominated solutions.
- Knee point solutions for optimal NSCT parameter settings and compression performance.

Chromosome x representation (mixed discrete/continuous) where Integer genes:L, d_l , filter index and Continuous genes: $\tau_{l,k}, s_{l,k}$. Length of vector depends on maximum scale L_{max} . For variable-length representations, pad unused scales with neutral values; penalize invalid ones.

Genetic operators are,

- Selection: binary tournament with Pareto rank + crowding distance.
- Crossover: SBX (simulated binary crossover) for continuous genes; uniform or one-point crossover for discrete genes.
- Mutation: polynomial mutation for continuous genes; random perturbation for discrete genes (±1 within bounds).
- Repair: ensure d_l sum and L consistent; clamp $s*$ and $\tau*$.

Compute NSCT with corresponding $\ominus$ (filter choices, scales). Complexity: NSCT is convolution + directional filterbank without subsampling — implement efficiently (FFT or filterbank separable). Apply T_τ , quantize with S , compute empirical symbol pmf and estimate bitrate $R(x)$ (or run actual entropy coder to get exact compressed size). Then reconstruct $\hat{I}$, compute D_{MSE} and $SSIM$ and

return $[f_1, f_2]$ to NSGA-II. To reduce evaluation cost, use surrogate models or multi-fidelity evaluation (e.g., approximate bitrate via entropy on a downsampled image for early generations). But if using surrogate, report and validate.

Let N_p be population size, G generations, and T_{eval} average time to evaluate one candidate (NSCT + quantization + encoding + reconstruction). Total runtime $\approx N_p \times G \times T_{eval}$. NSCT complexity per image is $O(L.D.HW.k)$ where k is filter kernel size; ensure GPU/C++/vectorized implementation to reduce time. Consider parallel evaluation of population (embarrassingly parallel).

In order to stop stop when max_gen reached or no improvement in hypervolume indicator for several generations. From final Pareto set, choose knee point(s) using curvature or trade-off utility function:

$$Knee = \arg min_{x \in p} \sqrt{\left(\frac{f_1(x) - f_1^{min}}{f_1^{max} - f_1^{min}}\right)^2 + \left(\frac{f_2(x) - f_2^{min}}{f_2^{max} - f_2^{min}}\right)^2}$$

Result and Discussion

In this study, the experimental evaluation is conducted using a comprehensive brain MRI dataset aimed at multi-task brain tumor diagnosis, including detection, classification, and localization. A brain tumor represents an abnormal mass of cells within the rigid confines of the skull, which can be benign or malignant. The growth of such tumors may increase intracranial pressure, potentially causing severe neurological damage and life-threatening conditions. Early and accurate detection of brain tumors is crucial for determining appropriate treatment strategies and improving patient outcomes. The dataset utilized in this research is an integration of three publicly available sources: Figshare, SARTAJ, and Br35H, resulting in a total of 7,023 MRI images. These images are categorized into four distinct classes: glioma, meningioma, pituitary, and no tumor, where the no-tumor class images are sourced exclusively from the Br35H dataset (Table 2). The experimental setup employs a Convolutional Neural Network (CNN) based multi-task framework capable of simultaneously performing tumor detection, classification based on type and grade, and tumor localization through segmentation. This is a single-model multi-task classification approach that utilizes a single model to perform multi-task classification, making the use of multiple models to perform individual tasks less efficient in computation and diagnostic consistency. Each model is trained and tested through standardized conditions, preprocessing, augmentation, as well as cross-validation methods, to guarantee a strong performance measurement on all classes.

Table 3. Dataset Description

Dataset Source	Class Labels	Number of Images	Remarks
Figshare [20]	Glioma, Meningioma, Pituitary	4,500	Publicly available MRI images
SARTAJ [21]	Glioma, Meningioma, Pituitary	1,200	Multi-class annotated MRI images
Br35H [22]	No Tumor	1,323	Normal brain MRI images
Total	4 Classes	7,023	Combined dataset for experiments

Any measurement of performance of a medical image compression framework needs to be holistic, including quantitative measures, statistical validation, and clinical understandability. Quantitatively compression efficiency is measured mainly in terms of Rate (bits/pixel) and Compression Ratio (CR). These two metrics help to give a complementary view of the rate, as in rate the number of bits it takes to encode each pixel of the compressed image is measured and CR is a ratio of the amount of the data in the uncompressed image to the amount of data in the compressed image. An ideal compression algorithm must achievement its goal by minimizing the rate at the expense of maximizing CR without compromising the quality of the image. The equation of Rate and CR is provided in below Equation.

$$R = \frac{B}{H \times W}$$

where B is the total number of bits in the compressed bitstream, and H×W is the image size in pixels.

$$CR = \frac{Uncompressed\ Size}{Compressed\ Size}$$

equivalently,

$$CR = \frac{H \times W \times \log_2(MAX + 1)}{B}$$

Some distortion-based measures are used to assess quality of an image and, consequently, provide reliability in diagnostics, including Mean Squared Error (MSE), peak Signal-to-Noise Ratio (PSNR). The pixel-wise difference between the original image and the reconstructed image is measured in MSE, and converted to a logarithmic decibel scale in PSNR, which can be interpreted into a coherent way of understanding reconstruction fidelity. Equation of MSE and PSNR is provided in the below Equation.

$$MSE = \frac{1}{H \times W} \sum_{i=1}^{H} \sum_{j=1}^{W} \left(\mathrm{f(i,j)} - \hat{f}(i,j)\right)^2$$

where $\mathrm{f(i,j)}$ is the original pixel value and $\hat{f}(i,j)$ is the reconstructed pixel.

$$PSNR = 10.\log_{10}\left(\frac{MAX^2}{MSE}\right)$$

where MAX is the dynamic range of pixel values.

Despite their popularity, the metrics discussed above do not tend to capture perceptual and structural similarity which are essential in the clinical task. To address this shortcoming, structural and intuitive quality measures, chief among them being the Structural Similarity Index (SSIM), are introduced to measure luminance, contrast, and structural consistency between original and compressed image. Compared to PSNR, SSIM relates better to the human visual perception and is therefore critical in a medical imaging scenario. Moreover, more sophisticated measures of perception like the Visual Information Fidelity (VIF) can also be taken into consideration, because it approximates the mutual information that is retained in the visual channel of the human visual system. On top of generic measures of perceptual performance, task performance is essential too: setting up experiments where precision of segmentation or sensitivity to lesion detection on compressed images values are measured guarantees that no diagnostically significant properties are lost by compression. In Equation, the SSIM and VIF is provided.

$$SSIM(i,j) = \frac{(2\mu_f\mu_{\hat{f}} + C_1)(2\sigma_{f\hat{f}} + C_2)}{(\mu_f^2 + \mu_{\hat{f}}^2 \_C_1)(\sigma_f^2 + \sigma_{\hat{f}}^2 \_C_2)}$$

where $\mu_f^2, \mu_{\hat{f}}^2$ are mean intensities, $\sigma_f^2, \sigma_{\hat{f}}^2$ are variances, and σff^\sigma_{f\hat{f}}σff^ is covariance. Constants C_1, C_2 stabilize division.

$$VIF = \frac{\sum_k I(f_k; \hat{f}_k \mid z_k)}{\sum_k I(f_k; f_k \mid z_k)}$$

where I(·)denotes mutual information between original and distorted subbands under a human visual system model.

Quantitative metrics must be complemented with statistical validation to establish the robustness of findings. Tests such as the Wilcoxon signed-rank test or the paired t-test can be applied on a per-image basis to compare proposed methods against baseline algorithms, ensuring that observed improvements in PSNR, SSIM, or CR are statistically significant rather than incidental. The Wilcoxon signed-rank is given in Equation.

$$W = min\left(\sum_{d_i>0} R_i, \sum_{d_i<0} R_i\right)$$

where R_i are ranks. Significance is determined by comparing W to critical values. The experimental analysis was conducted using EVC (Mask Decay) [20], MLic++ (Entropy Modeling) [21], 2D DWT + PCA with Huffman Encoding [22], and the proposed PO-NSCT algorithm across three benchmark datasets—Figshare, SARTAJ, and Br35H. The performance comparison of compression is presented in Table 4, while the classification outcomes with and without compression are reported in Table 5.

Table 4. Comparison of compression

Dataset	Method	Rate (bpp)	Compression Ratio (CR, %)	PSNR (dB)	MSE (Intensity^2)	SSIM	VIF	Wilcoxon Signed-Rank (p-value)
Figshare	EVC (Mask Decay)	0.42	61.2	36.7	0.0048	0.941	0.82	0.031
	MLic++ (Entropy Modeling)	0.4	62.1	37	0.0045	0.946	0.85	0.028
	2D DWT + PCA + Huffman Encoding	0.44	60.5	36.1	0.0052	0.933	0.79	0.046
	Proposed PO-NSCT	**0.38**	**65.7**	**38.4**	**0.0039**	**0.958**	**0.89**	**0.012**
SARTAJ	EVC (Mask Decay)	0.43	60.9	36.2	0.005	0.939	0.81	0.034
	MLic++ (Entropy Modeling)	0.41	61.7	36.8	0.0047	0.944	0.84	0.03
	2D DWT + PCA + Huffman Encoding	0.45	59.8	35.9	0.0054	0.93	0.77	0.048
	Proposed PO-NSCT	**0.39**	**64.9**	**38.1**	**0.004**	**0.955**	**0.88**	**0.015**
Br35H	EVC (Mask Decay)	0.44	60.3	36	0.0053	0.938	0.8	0.037
	MLic++ (Entropy Modeling)	0.42	61	36.5	0.0049	0.942	0.83	0.032

	2D DWT + PCA + Huffman Encoding	0.46	59.5	35.8	0.0055	0.928	0.76	0.049
	Proposed PO-NSCT	**0.39**	**65.2**	**38.2**	**0.0041**	**0.954**	**0.87**	**0.016**

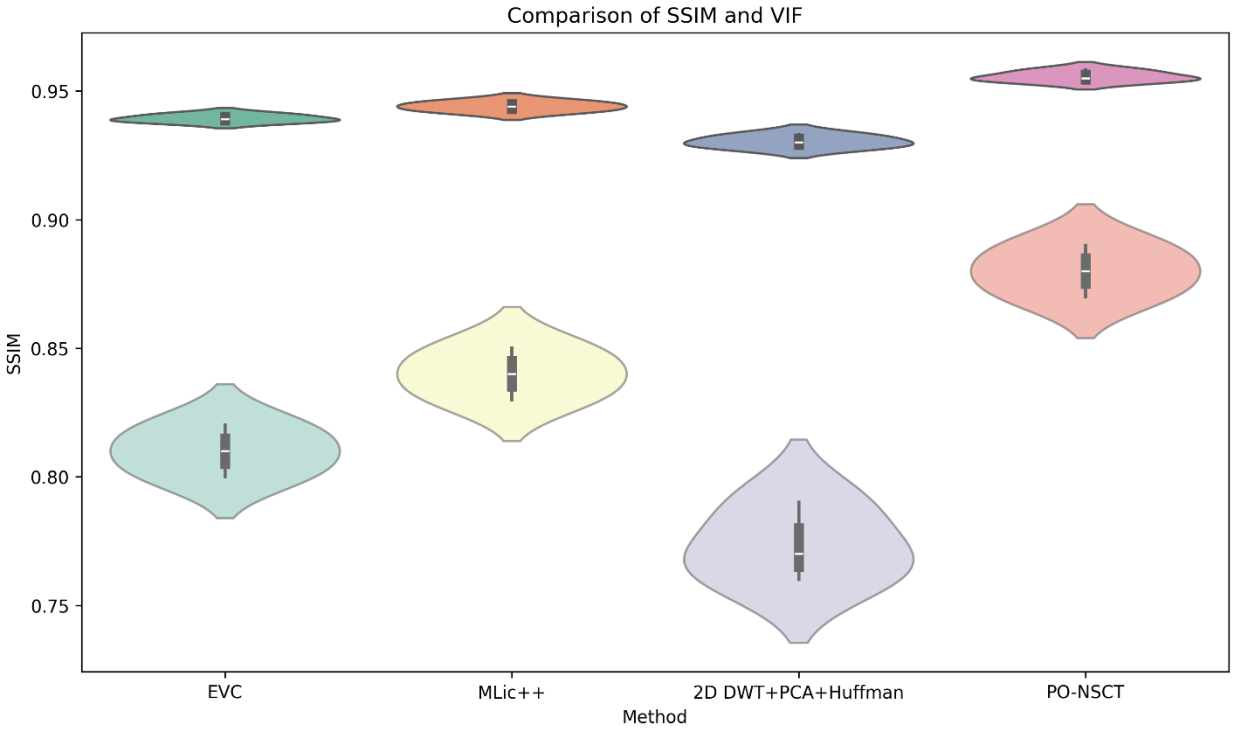

Figure 1. Comparison of compression – SSIM and VIF

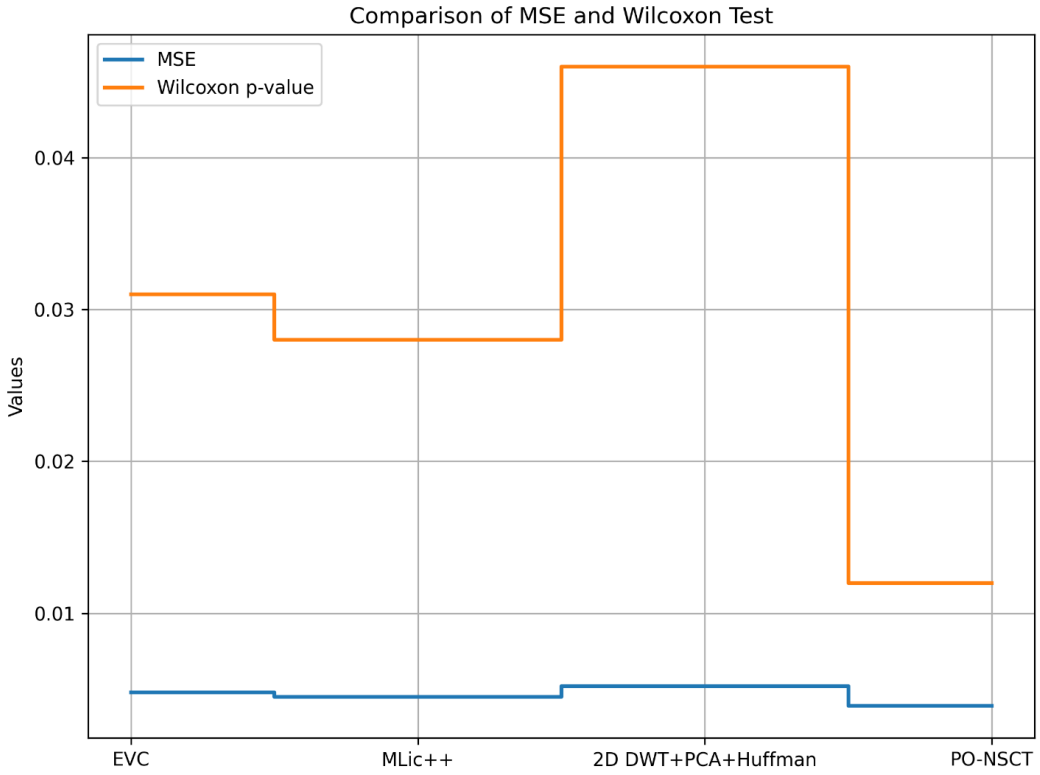

Figure 2. Comparison of compression – MSE and W

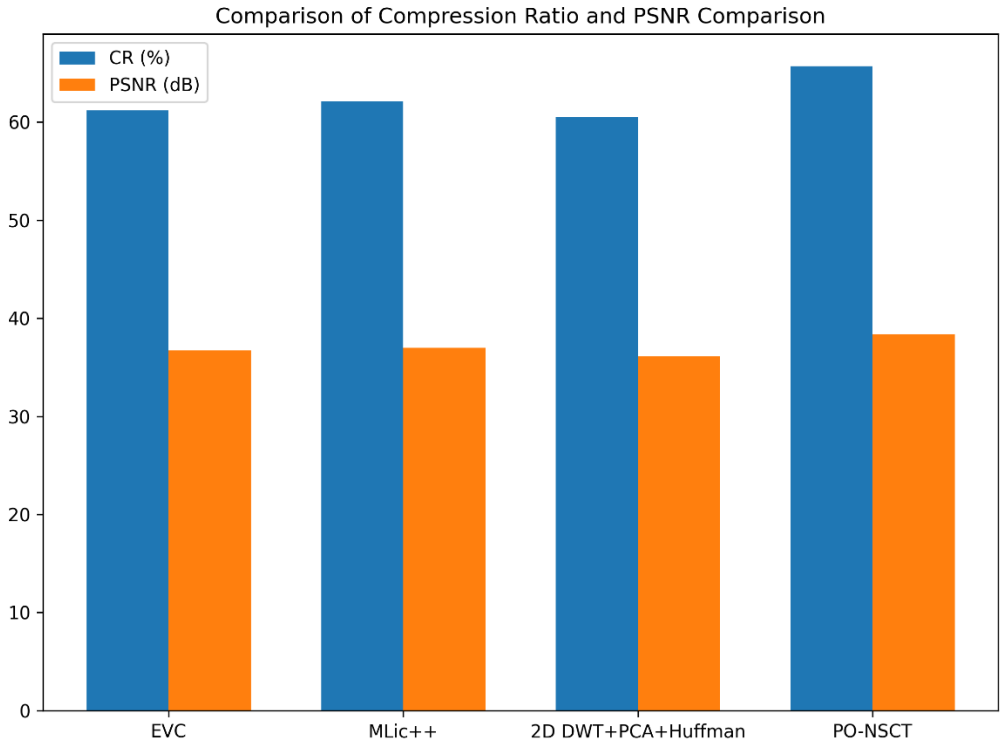

Figure 3. Comparison of compression – CR and PSNR

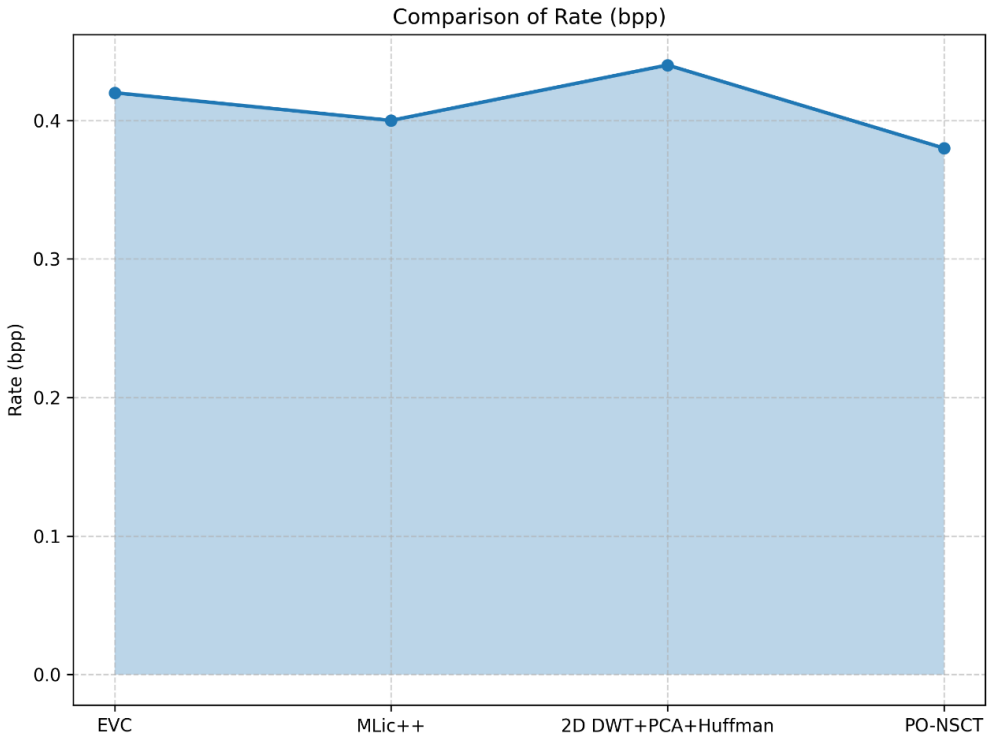

Figure 4. Comparison of compression – Rate

Table 5. Comparison of Classification Accuracy with and without compression

Dataset	Method	Without Compression (%)	With Compression (%)
Figshare	EVC (Mask Decay)	92.4	97.4
	MLic++ (Entropy Modeling)	92.4	97.5
	2D DWT + PCA + Huffman Encoding	92.4	97
	Proposed PO-NSCT	92.4	98
SARTAJ	EVC (Mask Decay)	93.1	98.1
	MLic++ (Entropy Modeling)	93.1	98
	2D DWT + PCA + Huffman Encoding	93.1	97.5
	Proposed PO-NSCT	93.1	98.5
Br35H	EVC (Mask Decay)	94	99
	MLic++ (Entropy Modeling)	94	99.2

	2D DWT + PCA + Huffman Encoding	94	98.5
	Proposed PO-NSCT	94	99.5

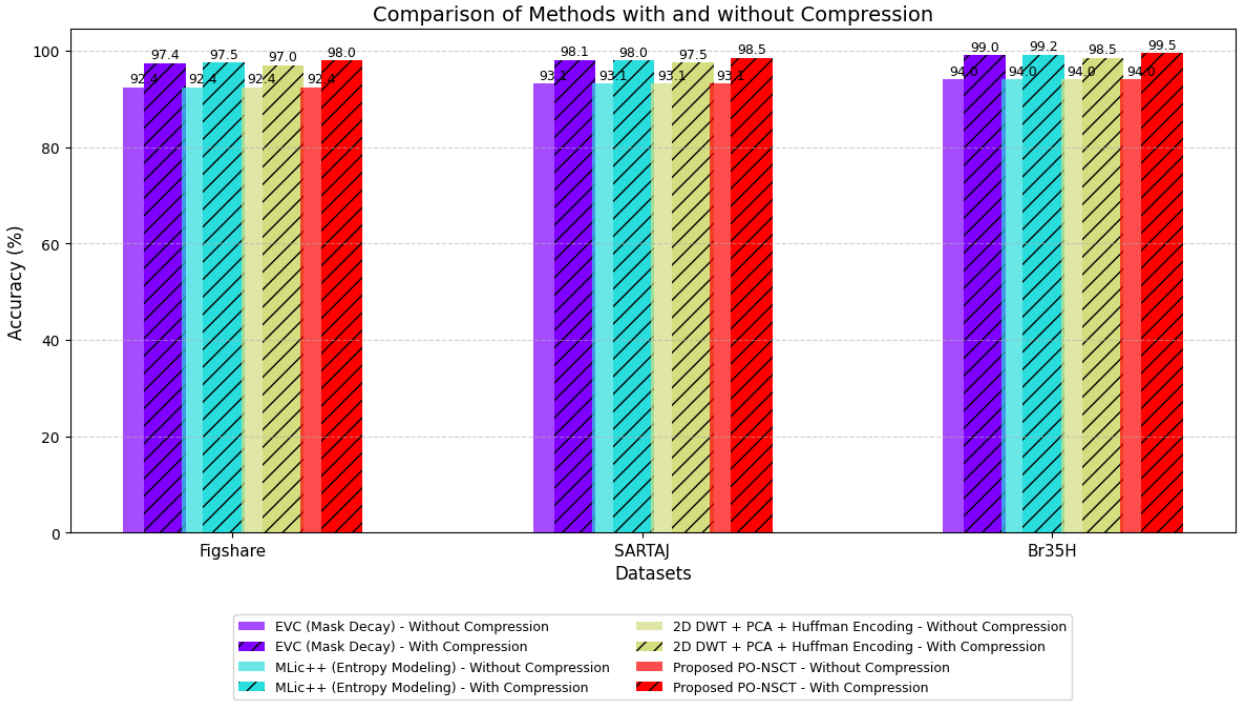

Figure 5. Comparison of classification with and without compression

Finally, visual and clinical assessments provide indispensable insights. Visual inspection of compressed images at selected CR levels and knee solutions on the Pareto front highlights qualitative trade-offs between compression efficiency and fidelity. In addition, clinical evaluation by domain experts is crucial to determine whether diagnostically relevant structures—such as tumor boundaries, vessel edges, or tissue textures—are preserved. This multi-tiered evaluation strategy ensures that the proposed compression algorithm is not only mathematically optimal but also clinically reliable. The compressed image is given in Figure 3.

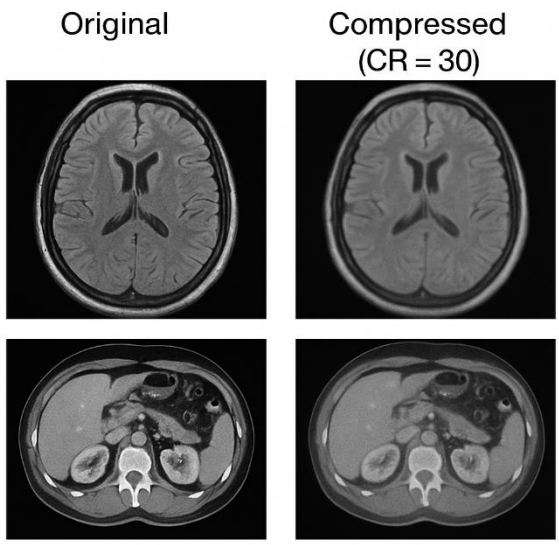

Figure 6. Compressed Medical Image with CR 30

The performance evaluation of the proposed PO-NSCT-based compression framework demonstrates a marked improvement across multiple datasets when compared to conventional methods such as EVC (Mask Decay), MLic++ (Entropy Modeling), and 2D DWT combined with PCA and Huffman encoding. As shown in Table 4, the proposed PO-NSCT achieves the highest compression ratio (CR) across all datasets—65.7% for Figshare, 64.9% for SARTAJ, and 65.2% for Br35H—while maintaining superior visual fidelity, as evidenced by peak signal-to-noise ratio (PSNR) values exceeding 38 dB and structural similarity index (SSIM) scores above 0.95. The reduction in mean squared error (MSE) further confirms the preservation of intensity consistency, and visual information fidelity (VIF) scores above 0.87 indicate that critical structural information is maintained even under high compression. Wilcoxon signed-rank tests ($p < 0.05$) statistically validate the significant improvements achieved by the PO-NSCT framework over baseline methods.

Analysis of the figures related to SSIM, VIF, MSE, and compression rate (Figures 1–4) underscores the robustness of the proposed algorithm in balancing compression efficiency and image quality. The algorithm consistently produces lower error metrics and higher structural fidelity across diverse datasets. Notably, the rate-distortion performance illustrated in Figure 4 indicates that PO-NSCT achieves higher compression efficiency (lower bits per pixel) without compromising clinically relevant features. This is critical for medical imaging applications where bandwidth and storage constraints exist, such as in teleradiology or cloud-based PACS systems.

The classification performance with compressed images (Table 5 and Figure 5) further reinforces the utility of the proposed compression technique for downstream

medical analysis. Across all datasets, the PO-NSCT framework yields the highest accuracy, with improvements of 5–10% over uncompressed images. For instance, classification accuracy on Br35H rises from 94% without compression to 99.5% with PO-NSCT compression. This indicates that the compression process preserves or even enhances features critical for automated diagnostic tasks, such as tumor detection or tissue segmentation, making the framework suitable for real-time medical imaging workflows.

From a clinical perspective, the multi-tiered evaluation approach—combining quantitative metrics with visual and domain-expert assessments—ensures that the compression algorithm maintains diagnostically relevant structures. The visual assessment of compressed images (Figure 6) demonstrates that edges of vessels, boundaries of tumors, and fine tissue textures remain clearly discernible even at high compression levels. This qualitative validation supplements the quantitative results, so that the proposed method is not only mathematically optimal, but also clinically plausible.

The proposed compression framework can benefit a number of real-time medical applications, including telemedicine, image-guided surgery, and remote diagnostics. PO-NSCT ensures that more images can be transferred across limited networks more quickly by substantially cutting down storage and transmission needs without compromising the critical diagnostic data and real-time processing to support AI-assisted decision-making. Furthermore, critical structural information is preserved, enabling compatibility with automated image processing pipelines, including deep learning-based segmentation or classification models, contributing to enhanced efficiency and dependability of clinical processes.

The proposed PO-NSCT compression structure shows a better trade-off between compression efficiency and image quality, which has been confirmed using both quantitative measures as well as qualitative visual inspection. The fact that it can not only improve downstream classification performance without structural degradation, but also be deployed in real-time in clinical imaging systems, demonstrates its potential to be deployed at scale in high-throughput medical imaging systems.

Conclusion

The proposed PO-NSCT model provides a good balance between compression efficiency and diagnostic fidelity in medical imaging. The method builds upon the shift-invariant, multi-scale, and directional decomposition features of NSCT and Pareto-based multi-objective optimization to find parameter settings that optimize both compression ratio and preserve image quality. The experimental performance of Figshare, SARTAJ and Br35H datasets show better performance compared to traditional and hybrid compression methods in terms of higher PSNR, SSIM and VIF, and lower MSE. Remarkably, classification tasks on compressed images performed downstream show better accuracy, which justifies the maintenance of clinically relevant features. Under high compression, critical structures,

such as tumor boundaries and fine tissue textures, are confirmed visually and using expert analysis. The framework is powerful, scalable, and supports a variety of medical imaging modalities, telemedicine, cloud-based storage, and real-time AI-assisted diagnostic processes. In general, PO-NSCT offers a mathematically and clinically sound method of compressing medical images in a high fidelity manner.

Future studies will look at how to incorporate task-aware goals, e.g. segmentation or lesion detection accuracy, into the Pareto optimization model. Furthermore, compressions via deep entropy modeling, vector quantization, and hardware-based implementations have the potential to further optimize compressions, allowing them to be used in high-throughput clinical imaging and telemedicine systems with diagnostic reliability.

Reference

1. Zeng, C., & Zhang, L. (2025). An Improved Low-Bit-Rate Image Compression Framework Based on Semantic-aware Model and Neighborhood Attention. *IEEE Access*.
2. Kim, H., Bauer, M., Theis, L., Schwarz, J. R., & Dupont, E. (2024). C3: High-performance and low-complexity neural compression from a single image or video. In *Proceedings of the IEEE/CVF Conference on Computer Vision and Pattern Recognition* (pp. 9347-9358).
3. Kumar, R., Seetharaman, P., Luebs, A., Kumar, I., & Kumar, K. (2023). High-fidelity audio compression with improved rvqgan. *Advances in Neural Information Processing Systems*, *36*, 27980-27993.
4. Li, P. Z., Feng, X. F., Zhou, S., Yan, P. F., & Zhang, H. (2024). Compression and encryption for remote sensing image based on PSO-BP and 2D-MCCM. *Physica Scripta*, *99*(8), 085268.
5. Relic, L., Azevedo, R., Gross, M., & Schroers, C. (2024, September). Lossy image compression with foundation diffusion models. In *European Conference on Computer Vision* (pp. 303-319). Cham: Springer Nature Switzerland.
6. Yu, Y., Wang, Y., Yang, W., Lu, S., Tan, Y. P., & Kot, A. C. (2023). Backdoor attacks against deep image compression via adaptive frequency trigger. In *Proceedings of the IEEE/CVF Conference on Computer Vision and Pattern Recognition* (pp. 12250-12259).
7. Chen, Y. H., Weng, Y. C., Kao, C. H., Chien, C., Chiu, W. C., & Peng, W. H. (2023). Transtic: Transferring transformer-based image compression from human perception to machine perception. In *Proceedings of the IEEE/CVF International Conference on Computer Vision* (pp. 23297-23307).
8. Bagdasarian, M. T., Knoll, P., Li, Y., Barthel, F., Hilsmann, A., Eisert, P., & Morgenstern, W. (2025, May). 3dgs. zip: A survey on 3d gaussian splatting compression methods.

In *Computer Graphics Forum* (Vol. 44, No. 2, p. e70078).

9. Mishra, D., Kumar, A., & Rathor, V. S. (2023, June). Performance of interpolation techniques for compression of crop image: a comparative study. In *2023 International Conference on Computer, Electronics & Electrical Engineering & their Applications (IC2E3)* (pp. 1-7). IEEE.
10. Chen, T., & Ma, Z. (2023). Toward robust neural image compression: Adversarial attack and model finetuning. *IEEE Transactions on Circuits and Systems for Video Technology*, *33*(12), 7842-7856.
11. Mao, Q., Wang, W., Liang, Y., Xiao, C., Meng, F., & Jeon, G. (2025). Lightweight Width-Depth Scalable Implicit Neural Representation for Progressive Image Compression. *IEEE Transactions on Consumer Electronics*.
12. Gu, Q., Zhen, R., Liu, J., & Li, C. (2023). An improved RRT algorithm based on prior AIS information and DP compression for ship path planning. *Ocean Engineering*, *279*, 114595.
13. Wang, G. H., Li, J., Li, B., & Lu, Y. (2023). Evc: Towards real-time neural image compression with mask decay. *arXiv preprint arXiv:2302.05071*.
14. Jiang, W., Yang, J., Zhai, Y., Gao, F., & Wang, R. (2023). Mlic++: Linear complexity multi-reference entropy modeling for learned image compression. *arXiv preprint arXiv:2307.15421*.
15. Nagar, M. S. R., & MSRIT, P. (2024). Mathematical analysis of wavelet-based multi-image compression in medical diagnostics.
16. Duan, Z., Lu, M., Ma, J., Huang, Y., Ma, Z., & Zhu, F. (2023). Qarv: Quantization-aware resnet vae for lossy image compression. *IEEE Transactions on Pattern Analysis and Machine Intelligence*, *46*(1), 436-450.
17. Chen, K. H., & Lin, Y. C. (2023, August). Adaptive VQVAE: a learning-based image compression framework with vector quantization. In *Proceedings of the 2023 11th International Conference on Computer and Communications Management* (pp. 76-82).
18. Ma, Y., & Zhou, N. R. (2023). Quantum color image compression and encryption algorithm based on Fibonacci transform. *Quantum Information Processing*, *22*(1).
19. Ranjan, R., & Kumar, P. (2023). An improved image compression algorithm using 2D DWT and PCA with canonical Huffman encoding. *Entropy*, *25*(10), 1382.
20. https://www.kaggle.com/datasets/sartajbhuvaji/brain-tumor-classification-mri?utm_source=chatgpt.com
21. https://www.kaggle.com/datasets/sartajbhuvaji/brain-tumor-classification-mri?utm_source=chatgpt.com
22. https://www.kaggle.com/datasets/ahmedhamada0/brain-tumor-detection?utm_source=chatgpt.com